ELSEVIER

Journal of Nuclear Materials 283–287 (2000) 1390–1395

journal of nuclear materials

www.elsevier.nl/locate/jnucmat

On the mechanisms associated with the chemical reactivity of Be in steam

D.A. Petti *, G.R. Smolik, R.A. Anderl

Fusion Safety Program, Idaho National Engineering and Environmental Laboratory (INEEL), P.O. Box 1625, Idaho Falls, ID 83415-3860, USA

Abstract

One safety concern surrounding beryllium as a plasma-facing material in a water-cooled Tokamak is steam interactions with hot beryllium and the production of significant quantities of hydrogen. We have tested several different product forms of Be with different densities and levels of porosity. Oxidation kinetics has been determined by measurements of hydrogen release with a mass spectrometer, volumetric measurements of the product gas and weight change of the sample. We discuss and compare with the literature the fundamental mechanisms and kinetics controlling the oxidation of Be in steam. Fully dense beryllium exhibits parabolic, linear and accelerating modes of oxidation as temperature increases from 450°C to 1200°C. The oxidation mechanisms and temperature trends are similar for other product forms. Oxidation rates are higher, however, when processing or annealing significantly increases the extent of interconnected porosity and consequently the effective surface area. The effective surface area as measured by BET surface analyses is a key parameter when comparing oxidation rates.

1. Introduction

One of the safety concerns surrounding beryllium as the first-wall plasma-facing material in a water-cooled first wall or divertor is the potential for steam interactions with hot beryllium which can produce significant quantities of hydrogen. We have tested the steam chemical reactivity of many forms of Be including fully dense and porous consolidated powder metallurgy (CPM) products, irradiated CPM product (both as-irradiated and post-irradiation–annealed) and plasma-sprayed [1–4] to better understand the safety implications of its use as a plasma-facing material. We used weight gain and hydrogen measurements based on mass spectrometry and volumetric displacement to measure reaction rates based on the system described in Ref. [5]. The purpose of this paper is to discuss in broad terms the experimental results to help elucidate mechanisms controlling the oxidation of Be in steam as a function of temperature, time, and morphology of the various types of Be.

The oxidation of a metal by a reactive gas has been of keen interest to material scientists and engineers over the past 50 years and has been the subject of textbooks [6,7]. Different types of growth laws (i.e., rate at which the oxide film or scale grows on the surface of the metal or alloy) have been observed experimentally and mechanisms have been put forth to describe the experimental results in terms of behavior at the atomic scale. Beryllium has been studied extensively for use in nuclear, chemical and aerospace applications dating back to the 1950s (for example see Refs. [8–20]). Much of this work is useful in helping us understand the mechanisms of steam-chemical reactivity of beryllium.

2. Chemical reactivity mechanisms

A compilation of the reaction rates based on initial geometric surface areas for dense CPM Be that we tested in 1992 and 1997 indicates three different regions of linear Arrhenius behavior: a low temperature regime (400–600°C), an intermediate temperature

* Corresponding author. Tel.: +1-208 533 4153; fax: +1-208 533 4207.

E-mail address: pti@inel.gov (D.A. Petti).

0022-3115/00/$ - see front matter
PII: S0022-3115(00)00299-3

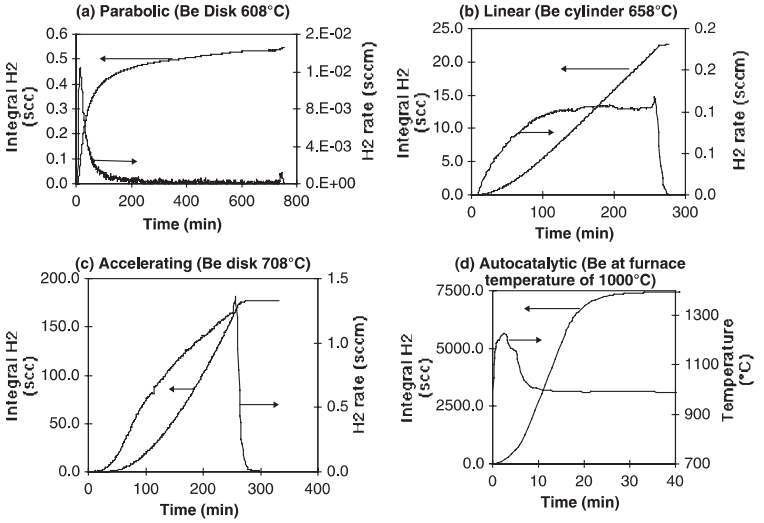

Fig. 1. Examples of different reaction kinetics observed in dense Be chemical reactivity testing.

regime (600–900°C) and a high temperature regime (900–1200°C).

In Fig. 1, we show different types of kinetic behavior observed during tests with dense Be. At low temperatures, reaction rates were parabolic (see Fig. 1(a)). At intermediate temperatures, we observed linear kinetics as indicated by the nearly constant reaction rate measured by the mass spectrometer (see Fig. 1(b)) or accelerating kinetics (see Fig. 1(c)) as indicated by the increase in the reaction rate measured by the mass spectrometer. At high temperatures, an autocatalytic reaction occurred increasing the temperature of the sample (see Fig. 1(d)).

The reaction kinetic behavior in these regimes and the implications on chemical reactivity mechanisms are discussed in Sections 2.1–2.3. Although we observed different reaction kinetics, we calculated effective linear rates based upon steam exposure times, total hydrogen generation as determined from cumulative plots and weight gain. Figs. 1(a) and (b) are plots that overlay the results of plasma-sprayed Be, irradiated Be, irradiated–annealed Be and porous Be with the dense Be plotted per unit of geometric surface area of the sample and per BET surface area. The reaction rates for these other forms of Be are much higher than the corresponding values for dense Be when plotted per unit geometric surface area. The chemical reactivity of these other forms of Be is a strong function of the specific surface area of these materials. Surface area considerations are discussed in detail in Section 2.4.

2.1. Low temperature regime

The detailed kinetic results suggest that different phenomena are controlling the overall oxidation process. In the low temperature region (<600°C), the reaction kinetics are generally parabolic. Numerous researchers have attributed parabolic oxidation kinetics at low temperatures in Be to diffusion of Be^{++} outward through the oxide scale to the surface for oxygen, nitrogen, and carbon dioxide [20,21]. This is because beryllium oxide is a semiconductor with cation conductivity [7]. Roth et al. [21] obtained an activation energy of 16.8 kcal/mol for Be^{++} diffusion through BeO. Results from our dense Be testing indicate an activation energy of 11.8 kcal/mol. The activation energy for the chemical reactivity of plasma-sprayed Be is 17.2 kcal/mol. These results are generally in good agreement.

We also observed that at these low temperatures, the overall oxidation was quite small, producing only a thin film, and the oxidation kinetics were a function of the surface finish. The chemical reactivity of our as-machined dense Be cylinders was somewhat greater than that of dense Be disks that were acid etched. We suspect that the as-machined surface contains a significant density of dislocations and other material damage at the surface that would affect the oxidation. This behavior is similar to that discussed by Papirov [20] in which he notes that surface roughness is governed primarily by the surface treatment of the sample and it exerts an influence on the growth of thin oxide films on Be in oxygen at 750°C.

2.2. Intermediate temperature regime

In the intermediate temperature range between 600°C and 900°C, the activation energy associated with the oxidation is larger. The reaction kinetics are complex and depends upon exposure time at a given temperature. There are indications of parabolic, linear, and

accelerating behavior (Figs. 1(a)–(c)). The linear oxidation kinetics indicate that the oxide layer is no longer protective and diffusion through the layer does not control the overall kinetics. Linear kinetics have traditionally been associated with metals where the specific volume of the oxide (m^3/kg) relative to the metal is either significantly less than or much greater than one [8]. For low specific volume ratios, the oxide cannot form a coherent film on the metal, whereas for high specific volume ratios, the film starts as coherent but then develops cracks or pores because of the stresses associated with the oxidation process. For Be, the volume ratio is ~1.7. Thus, there is significant volume expansion of the sample upon oxidation. The low plasticity of BeO and the stresses created during the oxidation process results in breakdown of a coherent BeO layer (via porosity and cracking) which would allow easy access of steam to a significant number of underlying sites such as inclusions and grain boundaries in the Be metal. This is consistent with the findings of Yoshida et al. [17] in which the oxide scale in their Be-steam experiments exhibited blisters and microcracks. There is an interesting time-dependent nature of the process. As the oxide cracks, heals, recracks and re-heals at different sites (and different times) in the sample, the kinetic behavior is the superposition of a number of small parabolic reactions, which is found to be linear when integrated over the entire sample. The accelerating behavior observed in some tests is associated with the creation of additional effective surface area from the diffusion of steam along the grain boundaries and formation of oxide along these sites on the surfaces. Grain boundary diffusion is generally much faster than bulk diffusion. Surface diffusivities are generally 10^5–10^6 times faster than bulk diffusivities [21,22]. The accompanying volume expansion induces stresses in the material that act as a wedge to force open the grain boundaries and expose new unreacted surface. This overall process increases the effective surface area for oxidation and leads to an accelerating reaction rate as shown in Fig. 1(c).

Others have also observed this behavior. Papirov [20] in his monograph notes that thin specimens were bent after testing in oxygen indicating the development of significant stresses in the oxide at 750°C. By 1050°C, the oxidation occurs predominantly along grain boundaries as confirmed by metallographic and X-ray studies. Tests in water vapor by Alymore et al. [11] show similar behavior above 650°C in which vigorous oxidation occurs along grain boundaries and the surface available for oxidation increases markedly. Thus, the overall kinetics are the superposition of two processes: surface oxidation and intergranular penetration, which predominates after oxide film breakdown. [20] Oxidation rates nearly become linear again at the advanced stages of accelerated oxidation. Consumption of metallic particles at the trailing edge and creation of new surfaces at the advancing edge of the oxide scale reach equilibrium. The metallographic cross-section of a sample we tested at 830°C illustrating such conditions is shown in Fig. 2.

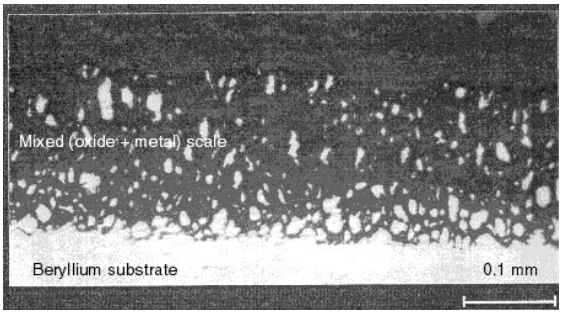

Fig. 2. Metallography of dense Be specimen showing steam penetration along grain boundaries producing a uniform reaction front.

2.3. High temperature regime

In the high temperature regime (>900°C), the temperature dependence of the overall reaction rate lessens relative to that in the intermediate regime as indicated by the decrease in slope, however, there is still some temperature dependence. As expected, the reaction rate is very high and significant consumption of the metal occurs. In some cases, the sample can experience autocatalytic behavior (Fig. 1(d)) and there can be gross changes in sample geometry up to a transformation including that of the dense Be sample into rubble.

Under this very rapid oxidation condition, it has been postulated that mass transport limitations become important. Blumenthal and Santy [19] in their work suggest that the change in the rate of reaction is due to hydrogen blockage of steam penetration through the porous oxide scale. The effect of a non-condensable gas like hydrogen on steam transport to a surface has been analyzed in the field of condensation mass transport [23]. The rate of steam transport follows traditional mass transport laws, but the rate of mass transfer is reduced because of the presence of the non-condensable gas. For reasonable values of the partial pressure of hydrogen at the surface (50–100% of bulk steam pressure) and in the bulk (10–1% of the bulk steam pressure), reduction in reaction rate can be a factor 2–10.

2.4. Surface area considerations

Other forms of beryllium [1–4] (plasma sprayed, irradiated Be, irradiated–annealed Be, and porous Be) that we have tested have shown enhanced reaction rates per unit of geometric surface area relative to dense Be.

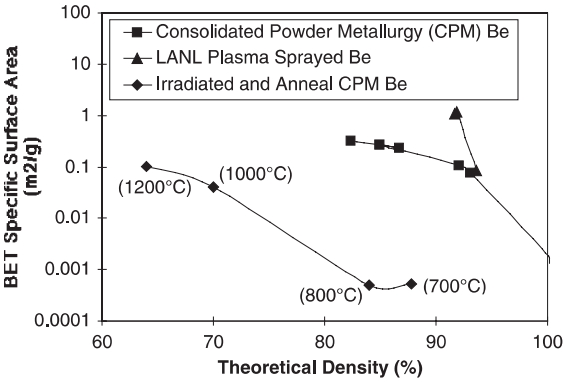

Fig. 3. BET specific surface area for different Be products.

These enhanced reaction rates are associated with the microstructure of the different forms of Be. Fig. 3 is a plot of the BET surface area for different forms of Be that we have tested. (BET is a gas adsorption technique to measure specific surface area [24].) Note that the plasma spray products show a strong dependence between theoretical density and specific surface area. The 92% dense plasma spray product has about an order of magnitude greater specific surface area than 92% dense Be, while the BET specific surface area of 94% dense plasma spray product is equivalent about to that of the CPM Be.

Irradiated Be that has been annealed above 1000°C also has a very high specific surface area relative to dense Be. Thermal anneals above 700°C in Be samples irradiated at 400°C to a fast neutron fluence of $5–7 \times 10^{21}$ n/cm^2 produced swelling between 15% and 55%. As shown in Fig. 4, during the anneal, the samples released tritium and helium concurrently. The swelling and the development of interconnected porosity associated with the post-irradiation annealing and

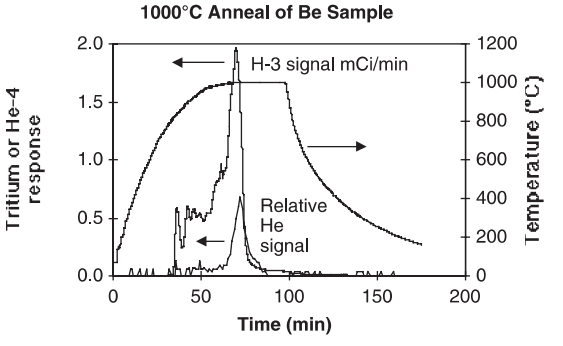

Fig. 4. Annealing of irradiated Be samples results in swelling, and after an incubation period development of interconnected porosity and simultaneous release of tritium and helium.

the subsequent tritium and helium release creates much more surface area relative to dense Be and provides for increased reaction rates when such a sample is exposed to steam.

Bennett et al. [15] observed similar behavior when they studied the oxidation behavior of irradiated Be in carbon dioxide. Oxidation rates in those experiments increased as a result of swelling and the development of a network of interconnected pores associated with liberation of helium. They noted that if the irradiated specimens are subjected to heat treatment in an inert atmosphere at a temperature sufficient to liberate helium from the Be matrix and to form pores, the oxidation even at low temperatures will be increased in proportion to the swelling and correlated with BET surface areas. Thus, our experiments reaffirm Bennett's contention [15] that the change in oxidation behavior in irradiated Be is not a change in the mechanism, but in the surface area available for reaction.

To illustrate the role of BET specific surface area in the oxidation behavior of Be in steam, we plot the reaction rate of the different forms of Be tested (plasma sprayed, irradiated, irradiated–annealed and porous) in terms of the total effective surface area, not the geometric surface area in Fig. 5(b). The results indicate that the chemical reactivity of the different forms of Be per unit surface area (as measured by BET) are very similar. Thus, the pre-existing effective surface area as determined by BET can explain, to a great extent, the differences in reaction rates measured for the different Be products.

3. Conclusions

The oxidation kinetics of Be-steam reactions between 400°C and 1200°C are quite complex. At low temperatures (<600°C), the reaction kinetics of dense CPM Be are parabolic suggesting that diffusion of Be^{++} through the oxide film is the rate controlling phenomena consistent with classic cation diffusion. At intermediate temperatures (600–900°C), the oxidation kinetics are varied and dependent on exposure time. Reaction kinetics are generally linear at lower temperatures in this range, but show accelerating behavior with longer times and higher temperatures. In the high temperature region (900–1200°C), the reaction rate is very high and significant consumption of the metal occurs. Some samples can experience autocatalytic behavior and gross changes in geometry. Some reduction in reaction rate could be expected because the steam must diffuse through the non-condensable hydrogen in the oxide pores and microcracks.

The effective surface area of the sample is very important in determining the chemical reactivity of Be in steam. The chemical reactivity of other forms of

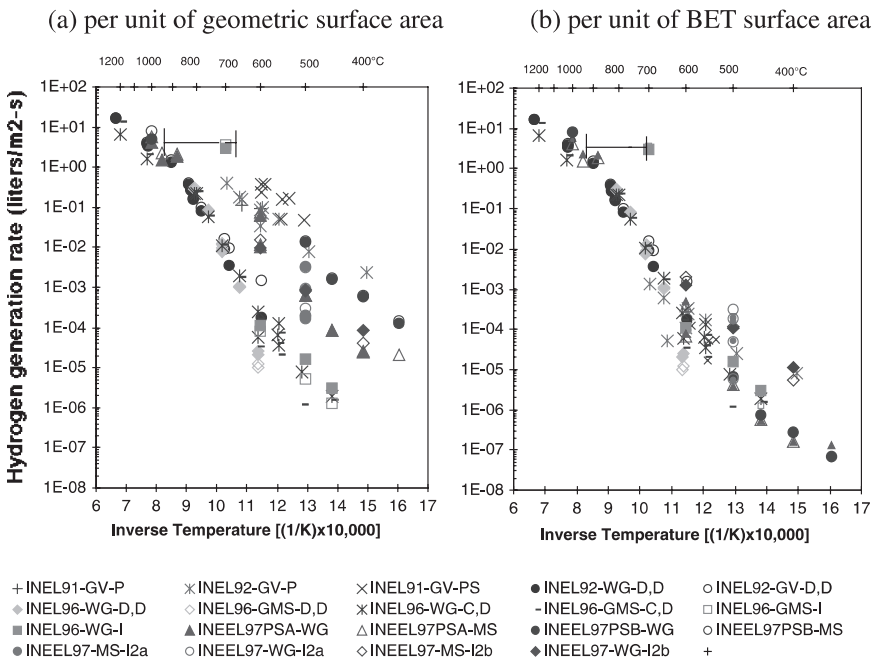

Fig. 5. Chemical reactivity of various forms of Be in terms of geometric and physical surface areas. (Different methods used to measure hydrogen are given by: GV – volumetric gas measurement of hydrogen; GMS or MS – mass spectrometer measurement of hydrogen; and WG – sample weight gain. Different types of Be include: P – porous; PS – plasma-sprayed; D,D – fully dense Be disk; C,D – fully dense Be cylinder; I – irradiated Be; PSA and PSB – plasma sprayed Be samples A and B from Los Alamos National Laboratory; and I2a and I2b – irradiated annealed Be.).

beryllium (plasma sprayed, irradiated Be, irradiated–annealed Be, and porous Be) that we have tested have shown enhanced reaction rates per unit of geometric surface area relative to dense Be. These enhanced reaction rates are associated with increased surface connected porosity of these different forms of Be. The chemical reactivities of the different forms of Be per unit surface area, as measured by BET, are very similar indicating that total surface area is a critical parameter in describing the oxidation behavior.

References

[1] R.A. Anderl et al., J. Fus. Energy 60 (1&2) (1997).
[2] R.A. Anderl et al., J. Nucl. Mater. 258–263 (1998).
[3] R.A. Anderl et al., Fus. Technol. 34 (1998) 738.
[4] G.R. Smolik, B.J. Merrill, R.S. Wallace, Reactions of Porous Beryllium in Steam, EGG-FSP-10346, July 1992.
[5] K.A. McCarthy, G.R. Smolik, R.A. Anderl, W.J. Carmack, G.R. Longhurst, J. Fus. Energy 60 (1&2) (1997).
[6] K. Hauffee, Oxidation of Metals, Plenum, New York, 1965.
[7] O. Kubaschewski, B. Hopkins, Oxidation of Metals and Alloys, 2nd Ed., Academic, London, 1962.
[8] D.W. White Jr., J.E. Burke, The Metal Beryllium, American Society of Metals, Cleveland, OH, 1955.
[9] The Metallurgy of Beryllium, Institute of Metals Monograph and Report Series No. 28, Chapman and Hall, London, 1963.
[10] D.W. Aylmore, S.J. Gregg, W.B. Jepson, J. Nucl. Mater. 2 (2) (1960) 160.
[11] D.W. Aylmore, S.J. Gregg, W.B. Jepson, J. Nucl. Mater. 3 (2) (1961) 190.
[12] S.J. Gregg, R.J. Hussey, W.B. Jepson, J. Nucl. Mater. 2 (3) (1960) 225.
[13] S.J. Gregg, R.J. Hussey, W.B. Jepson, J. Nucl. Mater. 3 (2) (1961) 175.
[14] S.J. Gregg, R.J. Hussey, W.B. Jepson, J. Nucl. Mater. 4 (1) (1961) 46.
[15] M.J. Bennett, N.W. Crick, P.B. Blythe, J.E. Antill, J. Nucl. Mater. 17 (1965) 60.
[16] I.B. Kupriyanov et al., in: Proceedings of the Second IAEA International Workshop on Beryllium Technology for Fusion, 6–8 September 1995, CONF-9509218, Idaho National Engineering Laboratory, September 1995.
[17] H. Yoshida, K. Ashibe, K. Ono, M. Enoeda, Measurements of Be Breakaway Reaction between Beryllium and Water Vapor for ITER Blanket Design, JAERI-M-92-083, June 1992.
[18] V.N. Chernikov et al., J. Nucl. Mater. 228 (1996) 47.
[19] J. Blumenthal, J. Santy, in: Proceedings of the 11th Symposium on Combustion, The Combustion Institute, Pittsburgh, Pennsylvania, 1967.
[20] I. Papirov, Oxidation and Protection of Beryllium, Edited Translation, FTD-HT-23-110-69, August 1969.

[21] J. Roth, W.R. Wampler, W. Jacob, J. Nucl. Mater. 250 (1997) 23.
[22] G.R. Holcomb, Corrosion 52 (7) (1996).
[23] J. Collier, Convective Boiling and Condensation, 2nd Ed., McGraw-Hill, New York, 1972.
[24] G.R. Smolik, R.A. Anderl, W.J. Carmack, P.B. Hembree, M.A. Oates, in: Proceedings of the 17th IEEE/NPSS Symposium on Fusion Energy, San Diego, CA, 6–9 October 1997.